Importance of carrier-carrier scattering for the ambipolar transport of optically generated carriers in a thin semiconductor slab

T. Kuhn and G. Mahler
Institut für Theoretische Physik, Universität Stuttgart, Pfaffenwaldring 57, D-7000 Stuttgart 80, Federal Republic of Germany
(Received 6 June 1988)

The ambipolar transport of an electron–hole–acoustic-phonon system in a semiconductor slab of some micrometers thickness is studied in an effective one-component model. Numerical solutions of the Boltzmann equation in relaxation-time approximation are given for different carrier-carrier scattering times $\tau_{c\text{-}c}$. Surprisingly, the resulting profiles of hydrodynamic variables (density, average velocity, and carrier temperature) are found to sensitively depend on this parameter. In the limiting cases of very weak, i.e., $\tau_{c\text{-}c}$ large compared with the carrier-phonon scattering time, or very strong carrier-carrier scattering, the profiles can be calculated to a good approximation in hydrodynamic models. In the latter case a nondiffusive velocity overshoot may occur. From the distribution function the line shape of the luminescence spectra is calculated as function of $\tau_{c\text{-}c}$ and slab thickness.

I. INTRODUCTION

During the last few years many experiments on the ambipolar transport of optically generated carriers have been performed, both under stationary excitation[1,2] and after generation by a short laser pulse.[3–7] In several cases, especially at low carrier densities, when exciton transport is dominant, it has been found[5,6] that experiments are in good agreement with simple theoretical calculations using the diffusion equation. Often, however, an additional velocity has been necessary to explain the results. There has been much controversy about the origin of this drift velocity. Steranka and Wolfe[3,4] found in their experiments velocities smaller or just below the sound velocity and thus favored the phonon wind as a driving force of the carrier system. Forchel *et al.*,[1] Schweizer *et al.*,[2] and Tsen *et al.*[7] needed drift velocities larger than the sound velocity to fit their spectra which thus excludes the phonon wind as the dominant effect. In this paper we investigate the influence of carrier-carrier scattering on stationary transport profiles and luminescence spectra and demonstrate that, due to surface effects and temperature gradients, high velocities are possible even without the nonequilibrium in the phonon system.

The various scattering processes in semiconductors can be divided into two classes: those processes leading to a relaxation of energy or momentum, e.g., electron-phonon or electron-impurity scattering, and those affecting only the shape of the distribution function without changing the hydrodynamic variables. Electron-electron and hole-hole scattering are examples of this second class, as well as exciton-exciton scattering, when exciton transport is considered. In many experimental situations only the behavior of hydrodynamic variables is studied; for example, an electric current density in presence of an electric field, a particle current density in presence of a density gradient, or an energy relaxation rate after excitation with a short light pulse. For this reason the two classes are often treated in a different manner in theoretical calculations. If the deviations from equilibrium are not too strong, electron-electron scattering can be neglected because it is a higher-order process for the calculation of conductivity or diffusion coefficient.[8] In the opposite case there are strongly driven systems with high density, where carrier-carrier scattering is the dominant process leading to a specific shape of the distribution function, e.g., heated and displaced Maxwellian or heated and displaced Fermi distribution. Instead of studying the whole distribution function, only the dynamics of a few functions of space and time, density, drift velocity, and carrier temperature, has to be calculated.

Carrier-carrier scattering is a two-particle process and thus dependent on density. This leads to the existence of parameter regions, where neither of these approximations is applicable. When density decreases, the carrier-carrier scattering time increases and may become comparable to carrier-phonon or carrier-impurity scattering in a certain density region. In this case both processes have to be treated on the same level and, as in other fields of physics, where length or time scales of different processes become comparable, interesting crossover effects can be expected.

In a previous paper[9] (hereafter cited as I) we studied the perpendicular transport of an optically generated ambipolar plasma in a thin semiconductor slab within a kinetic model. The main issues addressed have been the influence of the boundary conditions and the increase of a ballistic contribution when the transit time of the generated carriers becomes comparable to the momentum relaxation time. In this paper we demonstrate the importance of carrier-carrier scattering for calculations of the stationary profiles of density, average velocity, and temperature of the plasma. Because these variables are usually not directly measurable in an experiment we also present the optical spectra due to recombination.

II. KINETIC MODEL.

In order to avoid the problems arising from the two-component nature of the electron-hole plasma in a semi-

conductor, we use the same model semiconductor already discussed in I, where the masses and relaxation rates for electrons and holes are taken to be equal, reducing the problem to an effectively one-component system which is described by the stationary Boltzmann equation

$$\frac{\hbar k_z}{m}\frac{\partial}{\partial z}f(\mathbf{k},z)=g(\mathbf{k},z)+\left[\frac{\partial f}{\partial t}\right]_{c\text{-}p}+\left[\frac{\partial f}{\partial t}\right]_{c\text{-}c}. \tag{1}$$

Here, $g(\mathbf{k},z)$ is the generation rate due to the absorption of the laser light which creates carriers at a fixed excess energy $E_{\rm exc}$ above the band edge:

$$g(\mathbf{k},z)=\gamma e^{-\lambda z}\delta(\hbar^2k^2/2m-E_{\rm exc}) . \tag{2}$$

$(\partial f/\partial t)_{c\text{-}p}$ and $(\partial f/\partial t)_{c\text{-}c}$ are the collision operators for carrier-phonon and carrier-carrier scattering, respectively. We treat both processes in relaxation-time approximation. $(\partial f/\partial t)_{c\text{-}c}$ drives the distribution function towards a heated and displaced Maxwellian $f^c(\mathbf{k},z)$, where the carrier temperature T_c and drift velocity v_d have to be determined self-consistently from the distribution function. $(\partial f/\partial t)_{c\text{-}p}$ leads to a relaxation towards a nondisplaced Maxwellian at lattice temperature $f^L(\mathbf{k},z)$:

$$\left[\frac{\partial f}{\partial t}\right]_{c\text{-}p}=-\frac{1}{\tau_{c\text{-}p}}[f(\mathbf{k},z)-f^L(\mathbf{k},z)] , \tag{3a}$$

$$\left[\frac{\partial f}{\partial t}\right]_{c\text{-}c}=-\frac{1}{\tau_{c\text{-}c}}[f(\mathbf{k},z)-f^c(\mathbf{k},z)] . \tag{3b}$$

The hydrodynamic variables are given by

$$n(z)=\int f(\mathbf{k},z)d^3k , \tag{4a}$$

$$n(z)v_d(z)=\frac{\hbar}{m}\int k_z f(\mathbf{k},z)d^3k , \tag{4b}$$

$$\tfrac{3}{2}n(z)k_B T_c(z)=\frac{\hbar^2}{2m}\left[\int\left[k_z-\frac{m}{\hbar}v_d\right]^2 f(\mathbf{k},z)d^3k + \int k_{\parallel}^2 f(\mathbf{k},z)d^3k\right] , \tag{4c}$$

where $\mathbf{k}_{\parallel}=(k_x,k_y)$.

Integrating the Boltzmann equation (1) with respect to the parallel components of the momentum gives an equation for the one-dimensional distribution function f_0:

$$f_0(k_z,z)=\int f(\mathbf{k},z)d^2k_{\parallel} . \tag{5}$$

This function, however, is not sufficient for the calculation of the carrier temperature. The second integral in (4c) defines a parallel temperature which does not necessarily coincide with the temperature in the z direction. Thus we introduce the second moment of f with respect to $k_{\parallel}$:

$$f_2(k_z,z)=\int k_{\parallel}^2 f(\mathbf{k},z)d^2k_{\parallel} . \tag{6}$$

The differential equation for f_2 is obtained by multiplying (1) by $k_{\parallel}^2$ and integrating with respect to the parallel momentum. The "Boltzmann equations" for f_0 and f_2 together with the hydrodynamic variables (4) form a closed set of equations that has to be solved self-consistently.

At low temperatures, where only acoustic phonons have to be considered, the relaxation time $\tau_{c\text{-}p}$ is given by

$$\tau_{c\text{-}p}=(1.8\ \text{ns}\,\text{K}^{3/2})T_L^{-1}T_c^{-1/2} , \tag{7}$$

where T_L is the lattice temperature. The prefactor is chosen to reproduce the correct ambipolar diffusion constant for Si. The carrier-carrier relaxation time $\tau_{c\text{-}c}$ is varied in the calculations. The material parameters used in the calculations can be found in I. The influence of the surfaces is modeled by the momentum-independent reflection coefficients R_0 and R_L at the surfaces $z=0$ and $z=L$, respectively. $1-R_0$ and $1-R_L$ are thus the surface recombination probabilities for a carrier arriving at the surfaces. Bulk recombination could easily be included, but in indirect semiconductors like Si it is a slow process compared to surface recombination in all cases considered in this paper and thus negligible for transport calculations. Including carrier-carrier scattering, the Boltzmann equation is nonlinear even in relaxation-time approximation through the parameters T_c and v_d. Though it can be solved analytically in the spatially homogeneous case with an electric field,[10] spatially inhomogeneous problems can only be solved numerically. We use the iterative procedure explained in I.

Figure 1 shows the spatial profiles of the hydrodynamic variables density, average velocity, and carrier temperature for various carrier-carrier scattering rates in a 20-μm sample at lattice temperature of 5 K. The carriers are generated by a stationary laser beam with an excess energy of 50 meV. The reflection probabilities are[11] $R_0=1$, $R_L=0$. Without carrier-carrier scattering (solid lines) the density behaves approximately as should be expected in a diffusion process: it has its maximum where the carriers are generated and decreases monotonically with increasing distance from the irradiated surface. The temperature profile has virtually no gradient. With increasing carrier-carrier scattering rate the shape of the density profile becomes qualitatively different. When the scattering rates of carrier-phonon and carrier-carrier scattering become comparable ($\tau_{c\text{-}p}$ is here typically in the order of 100 ps), the maximum of the density begins to move from the surface into the sample, although there is still no surface recombination at the front surface. Because of the continuity equation the particle current density j must be constant everywhere outside the generation region. Thus the average velocity $v=j/n$ has to decrease when the density increases. Due to the totally reflecting surface at $z=0$, the velocity is zero at the boundary and positive everywhere inside the slab. A maximum of the density inside the sample thus leads to a maximum of the velocity between the surface and the density maximum. As can be seen in Fig. 1(b), the velocity at the maximum is nearly 1 order of magnitude larger when carrier-carrier scattering is dominant, compared to the velocity at the same distance without this scattering mechanism.

The possibility of a density gradient in the same direction as the current density, a "reverse diffusion," has been pointed out in earlier papers.[9,12] Its origin is a strong

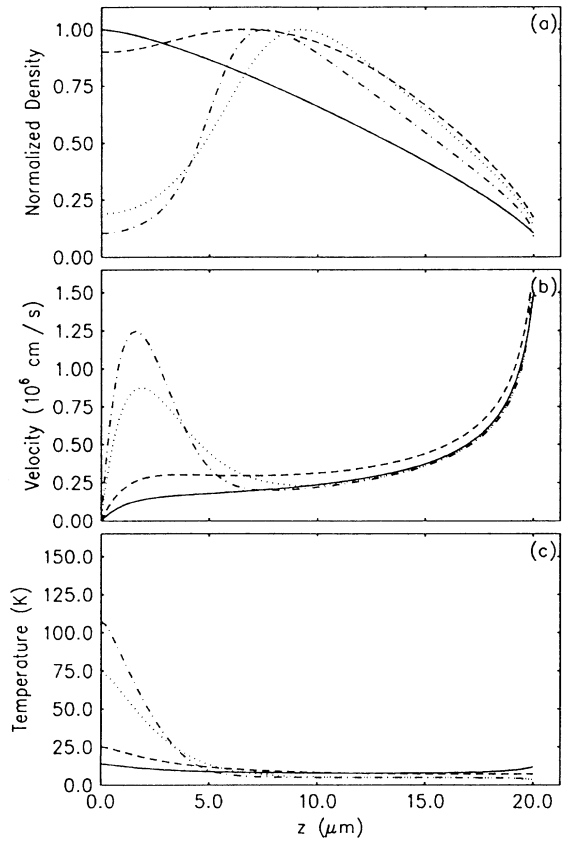

FIG. 1. (a) Density, (b) average velocity, and (c) carrier temperature profiles for $T_L = 5$ K, $E_{\text{exc}} = 50$ meV, $R_0 = 1$, $R_L = 0$ in a slab of 20 μm thickness with $\tau_{c\text{-}c} = \infty$ (solid lines), 100 ps (dashed lines), 10 ps (dotted lines), and 1 ps (dash-dotted lines), calculated within the kinetic model. $\tau_{c\text{-}p}$ in the order of 100 ps.

temperature gradient [Fig. 1(c)] leading to a strong energy current density and, by means of the thermodiffusion coefficient, also to a particle current density. If this current density becomes too large compared to the generation of new carriers by the laser light, a positive density gradient is built up to limit the current density. The temperature gradient, now, is strongly related to the carrier-carrier scattering rate. The carriers are always generated with an energy much larger than the mean energy at lattice temperature (~ 0.5 meV at 5 K compared to the excess energy of 50 meV). Without carrier-carrier scattering, those carriers with a small velocity component perpendicular to the surface remain in the generation region for a relatively long time, while the fast carriers are leaving this region leading to a narrow distribution function, which means a temperature which is small compared to the excess energy. Thus no strong temperature gradient can build up. On the other hand, with strong carrier-carrier scattering, the carriers are efficiently redistributed on small time scales. Total energy and momentum are conserved in this scattering process. The carrier temperature is mainly determined by the excess energy of the generation process. This leads to a strong temperature gradient between the surface and the bulk of the slab.

In Fig. 2 the hydrodynamic variables are plotted for different slab thicknesses. The carrier-carrier scattering time is 10 ps. Both surfaces are now totally absorbing, $R_0 = R_L = 0$. At a given slab thickness this gives the strongest nonequilibrium effects because the effective lifetime of the carriers inside the slab is the smallest. In the 5-μm slab the temperature never relaxes towards lattice temperature and there is no region of reverse diffusion. 10 μm is approximately the energy relaxation length and in the 20- and 30-μm slabs there is an increasing region of isothermal transport. Because of the longer effective lifetime in a thicker slab, the nonequilibrium effects (carrier temperature and average velocity) near the front surface become smaller with increasing thickness. If reverse diffusion occurs, the position of the density maximum is mainly given by the energy relaxation length, and for slabs thicker than this length it is approximately independent of thickness.

III. HYDRODYNAMIC MODELS

If one of the scattering processes is dominant and the thickness of the slab is large enough to ensure efficient

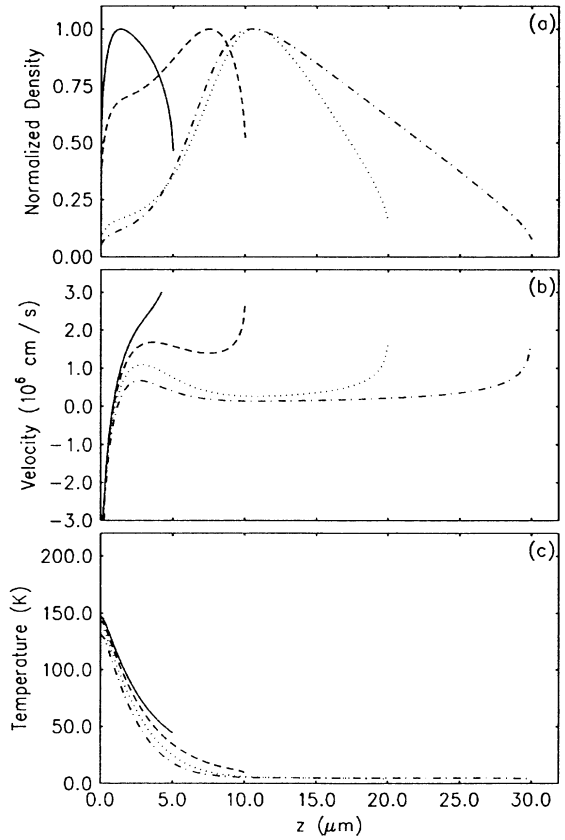

FIG. 2. Same as Fig. 1, but for $R_0 = R_L = 0$ and $\tau_{c\text{-}c} = 10$ ps in slabs of different thicknesses: 5 μm (solid line), 10 μm (dashed lines), 20 μm (dotted lines), and 30 μm (dash-dotted lines).

scattering before the carriers recombine at the surfaces, the shape of the distribution function can be parametrized by very few space-dependent variables. For $\tau_{c\text{-}p} \ll \tau_{c\text{-}c}$, carrier-carrier scattering can be neglected, since the equilibrium distribution for carrier-phonon scattering is also an equilibrium distribution for carrier-carrier scattering. The temperature is given by the lattice temperature and the system can be described by a simple diffusion equation for the carrier density n:

$$-\tau_{c\text{-}p}\frac{k_B T_L}{m}\frac{d^2 n}{dz^2}=G_0(z)\ . \tag{8}$$

G_0 is the carrier generation rate:

$$G_0(z)=\int g(\mathbf{k},z)d^3k = g_0 e^{-\lambda z}\ . \tag{9}$$

Since all equations are linear with respect to the density, the absolute value of g_0 is not important—the density scales with g_0.

In the opposite case, $\tau_{c\text{-}c} \ll \tau_{c\text{-}p}$, carrier-carrier scattering drives the shape of the distribution function towards a heated and displaced Maxwellian, but since this is not an equilibrium function for carrier-phonon scattering, that scattering mechanism leads to a relaxation of the average velocity and temperature. With the assumption of a heated and displaced Maxwellian, the Boltzmann equation (1) implies the following differential equations for density n, average velocity v, and carrier temperature T_c (given in terms of $\Theta = k_B T_c/m$):

$$\frac{dn}{dz}=\frac{1}{5\Theta-3v^2}\left[\frac{1}{v}\left[5\Theta G_0-G_2+\frac{3n}{\tau_{c\text{-}p}}(\Theta-\Theta_L)\right]-v\left[7G_0+4\frac{n}{\tau_{c\text{-}p}}\right]\right], \tag{10a}$$

$$\frac{dv}{dz}=\frac{1}{5\Theta-3v^2}\left[\frac{1}{n}(G_2+4v^2G_0)+\frac{1}{\tau_{c\text{-}p}}[4v^2-3(\Theta-\Theta_L)]\right], \tag{10b}$$

$$\frac{d\Theta}{dz}=\frac{1}{5\Theta-3v^2}\left[-\frac{\Theta}{nv}\left[5\Theta G_0-G_2+\frac{3n}{\tau_{c\text{-}p}}(\Theta-\Theta_L)\right]-\frac{v}{n}[G_2+(v^2-2\Theta)G_0]-\frac{v}{\tau_{c\text{-}p}}(v^2-2\Theta+3\Theta_L)\right], \tag{10c}$$

with

$$G_2=\frac{\hbar^2}{m^2}\int \mathbf{k}^2 g(\mathbf{k},z)d^3k=\frac{2}{m}E_{\text{exc}}G_0 \tag{11}$$

and $\Theta_L = k_B T_L/m$. G_2 is a measure of the energy associated with the generation of the carriers.

For unique solutions of the hydrodynamic equations (8) or (10) boundary conditions are necessary. Recombination at the surfaces leads to finite velocities of the carrier system at the boundaries, the well-known surface recombination velocities s_0 and s_L at the surfaces $z=0$ and $z=L$, respectively. With the assumption of an approximately unperturbed Maxwellian for the carriers moving towards the surface, density and current density at the surface can be calculated from the kinetic boundary conditions. Elimination of the density gives the surface recombination velocities

$$s_{0,L}=\left[\frac{2k_B T_c}{\pi m}\right]^{1/2}\frac{1-R_{0,L}}{1+R_{0,L}}\ . \tag{12}$$

The third condition for Eqs. (10) is the requirement that the variables are finite everywhere. (10a) and (10c) contain the average velocity v in the denominator. Since there is always one point inside the slab where the velocity is zero, the numerator of the respective terms must vanish at this point, leading to a connection between density and temperature at this point:

$$n=\frac{\tau_{c\text{-}p}}{3(\Theta-\Theta_L)}(G_2-5\Theta G_0)\quad \text{if } v=0\ . \tag{13}$$

The diffusion equation (8) can easily be solved analytically with the boundary conditions (12); Eqs. (10) together with the boundary conditions (12) and (13) have to be solved numerically. Figure 3 shows the profiles of the hy-

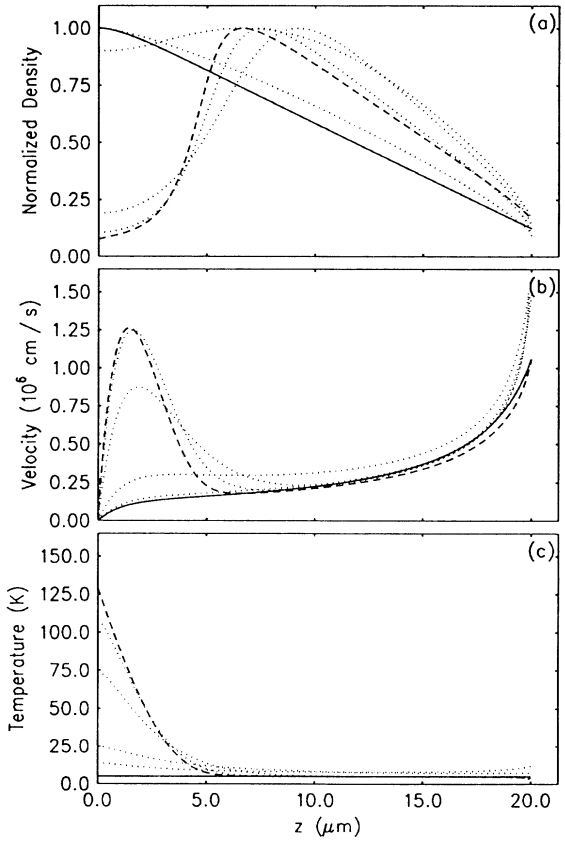

FIG. 3. (a) Density, (b) average velocity, and (c) carrier temperature for the parameters of Fig. 1 calculated within the isothermal diffusion model (solid lines) and the heated and displaced Maxwellian model (dashed lines). For comparison the profiles of the kinetic calculations are included as dotted lines.

drodynamic variables for isothermal diffusion (solid line) and for a heated and displaced Maxwellian (dashed line). For comparison the curves of Fig. 1 are included as dotted lines. The diffusion profiles are similar to the kinetic calculations without carrier-carrier scattering. The agreement is not perfect because, although there are no strong temperature gradients, the temperature is not exactly constant and it is everywhere somewhat larger than lattice temperature. The displaced Maxwellian calculation is in good agreement with the kinetic profiles for a carrier-carrier scattering time of 1 ps. Due to the higher temperatures near the surface, which lead to a smaller energy relaxation time (7), the density maximum is shifted to smaller z values. Because the heated and displaced Maxwellian is the limiting case of the distribution function for the infinite carrier-carrier scattering rate, scattering times below 1 ps will not lead to significant changes in the transport behavior inside the slab.

Near the surface $z=L$, the agreement, especially of the velocities becomes worse, because the boundary condition (12) has been derived under the assumption of a velocity small compared to the thermal velocity, which is not satisfied for a totally absorbing surface ($R_L=0$). Equation (12) always underestimates the true average velocity. In order to get a better expression for the boundary conditions, the Boltzmann equation (1) must be used to calculate the deviation of the distribution function from a heated and displaced Maxwellian in a small layer near the surface. This is just the Knudsen layer as introduced in gas-dynamic calculations and analyzed for the same geometry but different kinetic boundary conditions by Sone and Onishi.[13,14] A higher velocity at $z=L$ would result in slightly larger velocities everywhere inside the slab. This explains why the density maximum in the reverse diffusion region is not larger in the hydrodynamic calculations than for $\tau_{c\text{-}c}=1$ ps, as would be expected from the trend for decreasing $\tau_{c\text{-}c}$.

IV. LUMINESCENCE SPECTRA

Neither the full distribution function nor the space-dependent profiles of the hydrodynamic variables are directly measurable in an experiment. So one has to look for a quantity that is accessible by experiments and on the other hand provides enough information to get insight in the transport properties. The luminescence spectrum due to band-to-band recombination satisfies these requirements: in an indirect semiconductor it is a slow process which approximately does not influence the transport behavior in a thin slab and depends on the shape of the distribution function.

We assume that the optical dipole matrix element does not depend on the wave vector in the relevant region of $\mathbf{k}$ space where the distribution function is nonzero. In an indirect semiconductor, momentum is not conserved in a recombination process because of the participation of a phonon; thus, the luminescence intensity at frequency $h\nu$ is given by

$$I(h\nu)\sim\int d^3k\int d^3k'\int dz\, f_e(\mathbf{k},z)f_h(\mathbf{k}',z)\times\delta(h\nu-E_g-E_e(\mathbf{k})-E_h(\mathbf{k}'))\ , \tag{14}$$

where E_g is the gap energy, and E_e and E_h are the band-structures for electrons and holes, respectively. While for the calculations of the hydrodynamic variables from the Boltzmann equation only two moments of f with respect to the parallel momentum were sufficient, now the full dependence on $k_\parallel$ is needed. We approximate this dependence by a Maxwellian with the parallel temperature calculated from the second integral in (4c). Additionally, for the model semiconductor discussed in Sec. II the distribution function for electrons and holes are the same, thus

$$f_e(\mathbf{k},z)=f_h(\mathbf{k},z)=f_0(k_z,z)\left[\frac{\hbar^2}{2\pi m k_B T_\parallel}\right]\times\exp\left[-\frac{\hbar^2(k_x^2+k_y^2)}{2mk_BT_\parallel}\right]\ . \tag{15}$$

Inserting (15) in (14) the luminescence spectrum can now be calculated from the one-dimensional distribution function $f_0(k_z,z)$ according to

$$I(h\nu)\sim\int dk_z\int dk_z'\int dz\, f_0(k_z,z)f_0(k_z',z)[k_BT_\parallel(z)]^{-2}(\beta-k_z^2-k_z'^2)\exp\left[-\frac{\hbar^2}{2mk_BT_\parallel(z)}(\beta-k_z^2-k_z'^2)\right]\ , \tag{16}$$

with

$$\beta=(2m/\hbar^2)(h\nu-E_g)\ .$$

In Fig. 4 the luminescence spectra of the 20-μm slab are plotted for different carrier-carrier scattering times, the hydrodynamic profiles of which are those of Fig. 1. With decreasing scattering time the line first becomes broader and then narrower. This can be understood by inspection of the hydrodynamic variables: the distribution function enters quadratic in (16), thus the region of density maximum will dominate the spectrum. Without carrier-carrier scattering (solid line) the density maximum is at $z=0$. The velocity at this point is zero and the temperature is somewhat higher than lattice temperature. For $\tau_{c\text{-}c}=100$ ps (dashed line) the density remains nearly constant for about the first 6 μm. Temperature and average velocity are higher in this region than without carrier-carrier scattering, both leading to a broader spectrum. At lower scattering times (dotted and dash-dotted lines) the density maximum is inside the slab and, as already mentioned, due to the continuity equation the average velocity has a local minimum at this point. The temperature has nearly relaxed towards lattice temperature, so

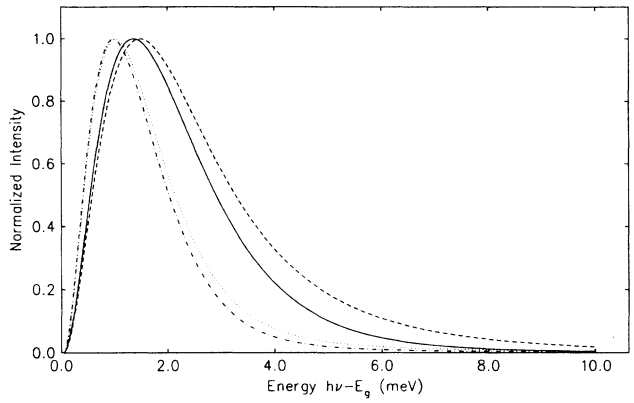

FIG. 4. Luminescence spectra for the profiles of Fig. 1. $\tau_{c\text{-}c}=\infty$ (solid line), 100 ps (dashed line), 10 ps (dotted line), and 1 ps (dash-dotted line).

the luminescence line is even narrower than without carrier-carrier scattering.

For the discussion of the luminescence spectra we referred only to the hydrodynamic profiles. An interesting question now is, whether this information might suffice even for the calculation of the spectra: We can construct a heated and displaced Maxwellian from the hydrodynamic variables and insert this distribution function in (14) to calculate the luminescence intensity. Motivated by the fact already discussed, that the point of density maximum will dominate the spectrum, we can try a still further simplification of the line-shape calculation: Instead of using the space-dependent heated and displaced Maxwellian we take only that one with temperature and drift velocity of the density maximum. In Fig. 5 these

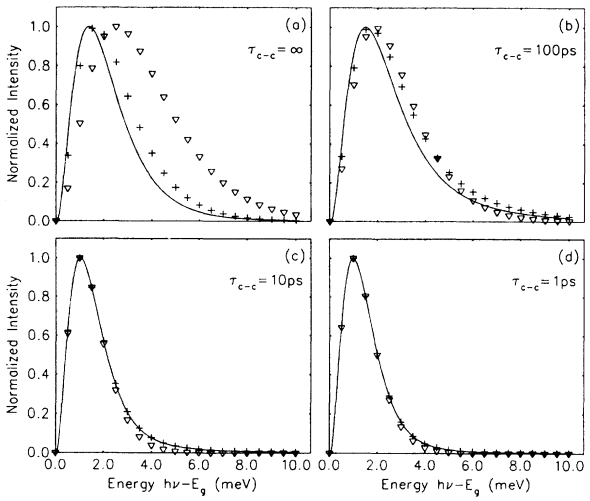

FIG. 5. Luminescence spectra for the parameters of Fig. 4 calculated from the full distribution function (solid lines), from a heated and displaced Maxwellian, where the hydrodynamic variables agree with the correct distribution function (+++), and from a single heated and displaced Maxwellian with the hydrodynamic variables at the density maximum of the kinetic calculation (∇∇∇).

two approximations are shown together with the kinetic result for the spectra of Fig. 4. Without carrier-carrier scattering [Fig. 5(a)] all three cases give different results. The spectrum with the exact distribution function is narrower than that with the space-dependent Maxwellian. Since carrier-phonon scattering is too small for a rapid thermalization of the carriers, the exact distribution function in the generation region is strongly affected by the generation rate $g(\mathbf{k},z)$. It contains carriers up to the excess energy which is large compared to $k_B T_L$. Thus the temperature of the corresponding Maxwellian is relatively high, giving a broader spectrum than the exact distribution function. The space-independent Maxwellian at the density maximum gives a much broader spectrum because the density maximum coincides with the temperature maximum, and the density is only slowly varying in a region where the temperature decreases. At small carrier-carrier scattering rates the increase of carrier temperature is mainly due to the parallel temperature. With respect to k_z the distribution function is relatively narrow because the carriers with large k_z are rapidly leaving the generation region, while those with large parallel momentum stay there, giving a large parallel temperature. At a carrier-carrier scattering time of 100 ps [Fig. 5(b)] the difference between the three cases is smaller than without this scattering mechanism, as it is expected for an increasing scattering rate. The exact distribution function still leads to a narrower line than the space-dependent Maxwellian, but now the space-independent Maxwellian is also in good agreement with the other cases since now the density maximum is inside the slab, where the temperature is slowly varying. At smaller scattering times [Figs. 5(c) and 5(d)] the space-dependent Maxwellian and the exact distribution function are in perfect agreement. Although the distribution function cannot be exactly a heated and displaced Maxwellian, since otherwise the hydrodynamic variables should be the same in both cases and agree with the solution of Eqs. (10) (see Fig. 3), the deviations are so small that they are not seen in the luminescence spectrum. The region of reverse diffusion increases the high-energy tail of the line because the high temperature and velocity in this region lead to recombination at photon energies where the density maximum gives only a small contribution. For $\tau_{c\text{-}c}=10$ ps this effect is stronger than for 1 ps because the density at the point of high velocities is larger.

The spectra corresponding to the thickness-dependent calculations of Fig. 3 are plotted in Fig. 6. In a thin slab the effective lifetime of the carriers is so small that energy and momentum can be very different from their equilibrium values. They are mainly determined by the excess energy of the laser. The line is very broad for the excess energy of 50 meV used in our calculations. With increasing thickness the line becomes narrower and in a slab thicker than the energy relaxation length (~ 10 μm) lattice temperature dominates the spectrum. At 20 μm there is still an appreciable deviation on the high-energy tail due to the high velocities and temperatures in the region near the front surface, while the 30-μm slab shows already a good agreement with an equilibrium spectrum at lattice temperature.

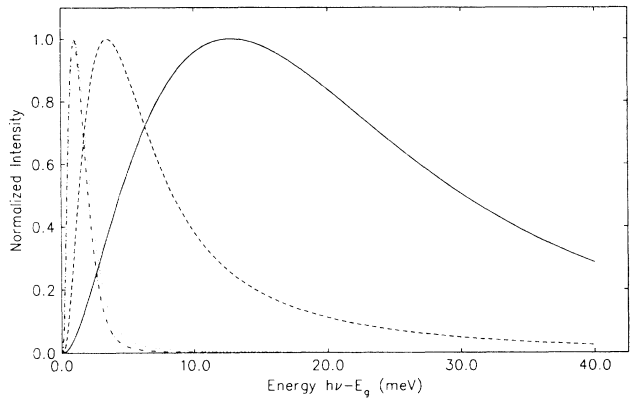

FIG. 6. Luminescence spectra for the thickness-dependent calculations with the parameters of Fig. 2. $L=5$ μm (solid line), 10 μm (dashed line), 20 μm (dotted line), and 30 μm (dash-dotted line).

V. CONCLUSIONS

We have demonstrated that the profiles of hydrodynamic variables (density, average velocity, and carrier temperature) depend strongly on the rate of carrier-carrier scattering, even though this scattering process cannot directly affect these variables. Without carrier-carrier scattering the system behaves approximately diffusively, and the density decreases monotonically with increasing distance from the generation region. When the carrier-phonon and carrier-carrier scattering rates become comparable, the density maximum begins to move away from the generation region. For $\tau_{c\text{-}c} \ll \tau_{c\text{-}p}$ the position of the density maximum is approximately constant, but the ratio between the density in the generation region and the maximum density decreases with decreasing $\tau_{c\text{-}c}$. This reverse diffusion is connected with a strong velocity overshoot at the end of the generation region. This overshoot behavior is, at first sight, counterintuitive, as one tends to expect scattering to impair rapid motion.

The physical reason for this effect is easily understood from the different temperature gradients. Only an efficient carrier-carrier scattering establishes a hot distribution function near the surface and thus a strong temperature gradient, because the energy relaxation length is approximately independent of $\tau_{c\text{-}c}$. If reverse diffusion occurs, the position of the density maximum is determined by this length. It does not depend on the sample thickness.

The limiting cases of very small or very strong carrier-carrier scattering can be described in hydrodynamic models, for $\tau_{c\text{-}p} \ll \tau_{c\text{-}c}$ by an isothermal diffusion and for $\tau_{c\text{-}p} \gg \tau_{c\text{-}c}$ by a heated and displaced Maxwellian. A major problem is the calculation of the hydrodynamic boundary conditions for the microscopic processes, which control the kinetic boundary conditions. Our simple model fails for average velocities comparable to or larger than the thermal velocity because it is well known that, in a layer of the mean free path of the carriers (the Knudsen layer in gas dynamics), the distribution function differs significantly from a displaced Maxwellian and depends on the carrier-carrier scattering rate. Nevertheless, the agreement between displaced Maxwellian and kinetic calculations for $\tau_{c\text{-}c}=1$ ps is very good in the major part of the slab.

The luminescence spectra also reflect the dependence on carrier-carrier scattering. For decreasing $\tau_{c\text{-}c}$ the line first becomes broader until both scattering mechanisms have approximately the same rate, because the temperature near the surface increases and the density is still high there. When $\tau_{c\text{-}c}$ is decreasing further the temperature at the surface is still rising, but the density is decreasing. At the position of the density maximum, which dominates the spectrum, the temperature has nearly relaxed towards lattice temperature, thus the spectrum now becomes narrower.

While for large $\tau_{c\text{-}c}$ the whole distribution function from the kinetic calculation is necessary to determine the luminescence spectrum accurately, below 10 ps it is practically perfectly reproduced, if a heated and displaced Maxwellian is used instead, where the hydrodynamic variables agree with the correct distribution function. For the main part of the luminescence line it is even a satisfying approximation to use just a single heated and displaced Maxwellian with temperature and drift velocity in agreement with those of the density maximum in the kinetic calculations. Only at the high-energy tail there is still a significant deviation due to the high temperatures and velocities in the reverse diffusion region.

In this paper we have restricted ourselves to the case of an excess energy smaller than the optical phonon energy. In most experimental situations this condition is not satisfied; the laser energy is much larger than the gap energy. Due to the high-energy relaxation rate in optical-phonon scattering, the carriers will lose their energy very fast until it is below the optical-phonon energy. The details of this process and the resulting density, velocity, and temperature profiles remain to be investigated. In kinetic calculations this is difficult because of the large number of iteration steps for fast scattering processes,[15] but the hydrodynamic description might be useful when carrier-carrier scattering is the fastest process. For a quantitative comparison with most experiments the degeneracy of the carrier system has also to be included in the calculations, but we expect that this does not qualitatively change our present results.

ACKNOWLEDGMENT

This work was supported by the Deutsche Forschungsgemeinschaft (Bonn, Germany) under Grant No. Ma-614/5-1.

[1]A. Forchel, H. Schweizer, and G. Mahler, Phys. Rev. Lett. **51**, 501 (1983).
[2]H. Schweizer and E. Zielinski, J. Lumin. **30**, 37 (1985).
[3]F. M. Steranka and J. P. Wolfe, Phys. Rev. Lett. **53**, 2181 (1984).
[4]F. M. Steranka and J. P. Wolfe, Phys. Rev. B **34**, 1014 (1986).
[5]G. Mahler, T. Kuhn, A. Forchel, and H. Hillmer, in *Optical Nonlinearities and Instabilities in Semiconductors*, edited by H. Haug (Academic, San Diego, 1988), p. 159.
[6]J. C. Culbertson, R. M. Westervelt, and E. E. Haller, Phys. Rev. B **34**, 6980 (1986).
[7]K. T. Tsen and O. F. Sankey, Phys. Rev. B **37**, 4321 (1988).
[8]J. Appel, Phys. Rev. **122**, 1760 (1961).
[9]T. Kuhn and G. Mahler, Phys. Rev. B **35**, 2827 (1987).
[10]N. S. Wingreen, C. J. Stanton, and J. W. Wilkins, Phys. Rev. Lett. **57**, 1084 (1986).
[11]The special case of a totally reflecting surface at $z=0$ has been chosen to demonstrate more clearly the effect of reverse diffusion. In a normal diffusion process the density maximum would then always be at the surface. For Si this is not an unrealistic case, since surface recombination velocities as small as 0.25 cm/s have been reported [E. Yablonovitch, D. L. Allara, C. C. Chang, T. Gmitter, and T. B. Bright, Phys. Rev. Lett. **57**, 249 (1986)]. With Eq. (12) this corresponds to $R_0 \approx 1-10^{-7}$.
[12]G. Mahler and A. Forchel, Helv. Phys. Acta **56**, 875 (1983).
[13]Y. Sone, J. Phys. Soc. Jpn. **45**, 315 (1978).
[14]Y. Onishi and Y. Sone, J. Phys. Soc. Jpn. **47**, 1676 (1979).
[15]The iterative solution of the Boltzmann equation is equivalent to the solution of the time-dependent problem in time steps Δt, where Δt has to be smaller than the smallest scattering time [W. Fawcett, in *Electrons in Crystalline Solids*, edited by A. Salam (IAEA, Vienna, 1973), p. 531]. The total time T necessary to establish a stationary distribution in a slab of thickness L is roughly given by $T=L/v_{\text{th}}$, where v_{th} is the thermal velocity of the carriers.